$La_2ZnGa_2S_6O$: A Melilite-Type Transition Metal Oxysulfide achieving a Well-Balanced Nonlinear-Optical Behavior

Jingjing Xu,[a] Yan Xiao,[b] Xiaowen Wu,[a,c,*] Bingbing Zhang,[b,*] Kui Wu[a,*]

a. State Key Laboratory of Crystal Materials and Institute of Crystal Materials, Shandong University, Jinan 250100, China. wukui@sdu.edu.cn

b. College of Chemistry and Materials Science, Hebei University, Baoding 071002, China. zhangbb@hbu.edu.cn

c. School of Resources and Environment Engineering, Shandong Agriculture and Engineering University, School of Resources and Environment Engineering, Shandong Agriculture and Engineering University.wuxiaowen1114@163.com

CONTENTS

1. Synthesis of Title compound.

All raw materials with high purity (>99.9%) were directly purchased from Beijing Hawk Technology Co., Ltd. To ensure the stability of raw materials and eliminate the effect of air oxidation on the La_2S_3, a vacuum glovebox was used to complete the whole weighing process. Single crystals of $La_2ZnGa_2S_6O$ were synthesized with the stoichiometric ratio based on the raw materials of La_2S_3, ZnO and Ga_2S_3 (1:1:1). The mixed and grounded raw materials were firstly placed into the vacuum-sealed silica tubes. A flame gun and vacuum pump were used to obtain a 10^{-3} Pa vacuum inside the silica tubes, and vacuum sealing was performed. Finally, the crystallization reaction of the title compounds was completed using a muffle furnace with the following temperature setting process: heating up to 1273K within 35 h and hold for 90 h, then cooling to room temperature within 150 h. Finally, the synthesis yielded a high yield (>95%) of the yellow-colored $La_2ZnGa_2S_6O$ crystals were obtained.

2. Structural Refinement and Crystal Data.

Selected high-quality crystals were collected using a Bruker D8 VENTURE diffractometer with Mo Kα radiation (λ = 0.71073 Å) at room temperature. Crystal structures were solved by the direct method, with absorption correction using a multiscan method and refinement using the SHELXTL program package. Detailed refinement parameters and data are shown in Table S2.

3. Property Characterization

3.1. Powder X-ray Diffraction.

Powder X-ray diffraction (PXRD) patterns were collected on a LANScientific fringe class with Cu Kα radiation (λ = 1.5418 Å) at room temperature. The 2θ range was 10-70° with a step size of 0.02° and a fixed counting time of 1s/step. The calculated XRD spectra originated from the corresponding single crystal data. We have compared the experimental and calculated XRD patterns of the title compounds.

3.2. UV−Vis−Near-IR (NIR) Diffuse Reflectance Spectra.

Diffuse reflectance spectra were measured in the wavelength range of 200-1400 nm at room temperature with a Shimadzu SolidSpec-3700DUV spectrophotometer.

3.3. Raman Spectra.

Hand-picked crystals were placed on a glass slide, and the Raman spectra were recorded using a an iHR550 Raman spectrometer equipped with a CCD detector by a 632nm He-Ne laser (5 mW).

3.4. Second-harmonic Generation Measurement.

Through the Kurtz and Perry method, powder SHG responses were investigated by a Q-switch laser (2.09 μm, 3 Hz, 50 ns) with different particle sizes, including 38−55, 55−88, 88−105, 105−150, 150−200, and 200−250 μm. As-synthesized $AgGaS_2$ microcrystals were ground and sieved into the same size ranges as the references.

3.5. Computational Description.

The first-principles calculation was carried out using the CASTEP package based on density functional theory (DFT) to further investigate the structure−property relationship. The Perdew−Burke−Ernzerhof (PBE) functional in the generalized gradient approximation (PBE-GGA) was used to describe the exchange-correlation energy. To achieve energy convergence, the plane-wave basis set energy cutoff is chosen to be 660 eV in the normal-conservation pseudopotential (NCP). As key parameters for NLO crystals, the birefringence was also calculated. Owing to the discontinuity of exchange correlation energy, the experimental value is usually larger than that of the calculated band gap. Thus, scissors operators are used to make the conduction bands agree with the experimental values. The SHG density of $La_2ZnGa_2S_6O$ were also calculated.

4. Tables and Figures

Table S1. Summary of the crystal structure data and NLO properties of reported NLO melilite-type transition metal oxysulfides.

Table S2. Crystal data and structure refinement for title compound.

Table S3. Calculation of dipole moment of $La_2ZnGa_2S_6O$ and $Sr_2ZnGe_2S_6O$ groups.

Figure S1. The structure of melilite-type $A_2M^{I}N^{II}_2Q_7$.

Figure S2. Calculated IR spectra for $La_2ZnGa_2S_6O$.

Table S1. Summary of the crystal structure data and NLO properties of reported NLO melilite-type transition metal oxysulfides.

Compound	Space group	Bandgap (eV)	SHG	Mixed-anion Units
$Sr_2CdGe_2S_6O$[1]	$P\bar{4}2_1m$	3.62	0.8×AGS	$GeOS_3$; $SrOS_7$
$Sr_2MnGe_2S_6O$[1]	$P\bar{4}2_1m$	3.51	0.3×AGS	$GeOS_3$; $SrOS_7$
$Sr_2ZnGe_2S_6O$	$P\bar{4}2_1m$	3.73	0.6×AGS	$GeOS_3$; $SrOS_7$
$Sr_2ZnSn_2S_6O$[2]	$P\bar{4}2_1m$	3.52	0.7×AGS	$GeOS_3$; $SrOS_7$
$Sr_2CoGe_2S_6O$[3]	$P\bar{4}2_1m$	2.77	0.34×AGS	$GeOS_3$; $SrOS_7$
$Sr_2FeGe_2S_6O$[4]	$P\bar{4}2_1m$	2.24	0.5×AGS	$GeOS_3$; $SrOS_7$
$Eu_2MnGe_2S_6O$[5]	$P\bar{4}2_1m$	2.40	0.3×AGS	$GeOS_3$; $EuOS_7$
$Eu_2FeGe_2S_6O$[5]	$P\bar{4}2_1m$	2.11	0.3×AGS	$GeOS_3$; $EuOS_7$
$Eu_2CoGe_2S_6O$[5]	[1]$P\bar{4}2_1m$	2.14	0.5×AGS	$GeOS_3$; $EuOS_7$

Table S2. Crystal data and structure refinement for title compound.

Empirical formula	$La_2ZnGa_2S_6O$
Formula weight	690.99
crystal system	*Tetragonal*
space group	P-42_1m
a (Å)	9.369 (3)
c (Å)	6.067(3)
Z, V (Å^3) (volume)	2, 532.6(4)
D_c (g/cm^3) (calculated density)	4.309
μ (mm^{-1}) (absorption coefficient)	16.179
goodness-of-fit on F^2	1.042
R_1, wR_2 (I>2σ(I))^a	0.0255, 0.0575
R_1, wR_2 (all data)	0.0277, 0.0585
Flack parameter	0.01(3)
Largest diff. peak and hole (e Å^{-3})	1.906, -1.023

Table S3. Calculation of dipole moment of $La_2ZnGa_2S_6O$ and $Sr_2ZnGe_2S_6O$ groups.

Compound	Unit	$d_{average}$	Δd	Δn
$La_2ZnGa_2S_6O$	ZnS_4	2.2867	0	0.120
	GaS_3O	2.1663	4.6712	
	LaS_7O	2.9798	2.4517	
$Sr_2ZnGe_2S_6O$[1]	ZnS_4	2.3366	0	0.114
	GeS_3O	2.1072	5.2517	
	SrS_7O	3.0578	0.8577	

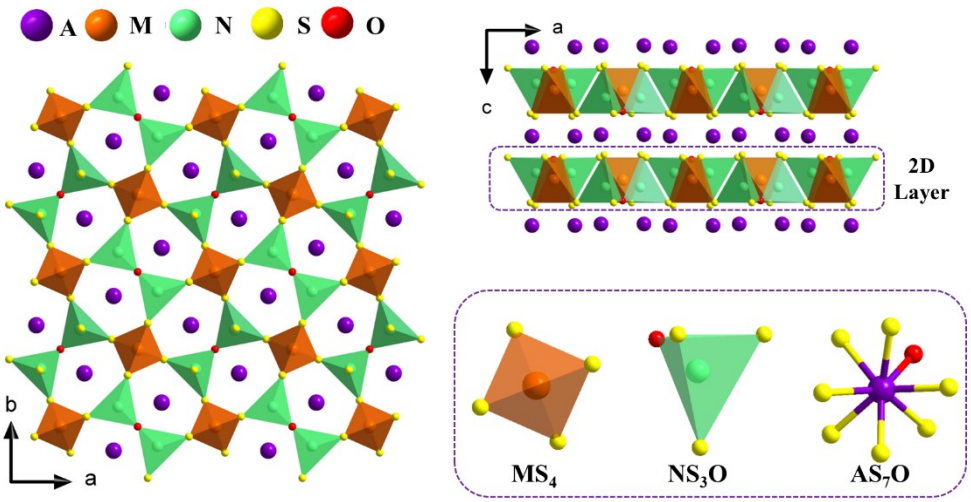

Figure S1. The structure of melilite-type $A_2M^{I}N^{II}_2Q_7$.

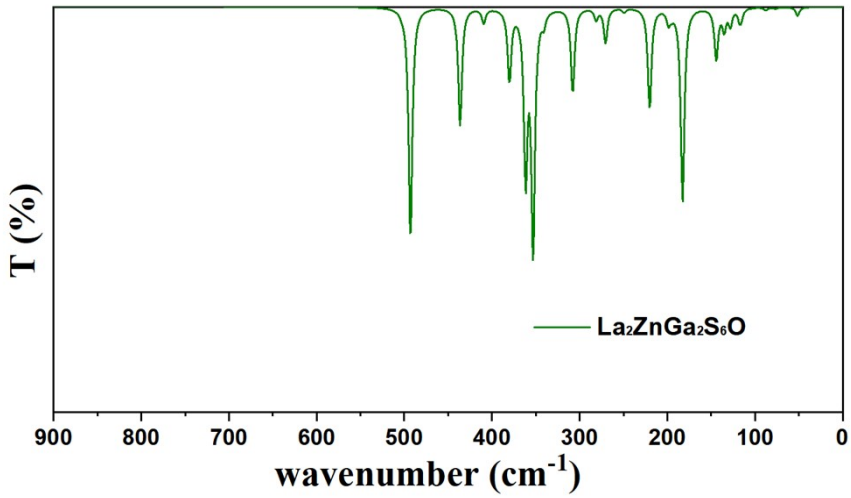

Figure S2. Calculated IR spectra for $La_2ZnGa_2S_6O$.

5. References

1. M.-Y. Ran, S.-H. Zhou, B. Li, W. Wei, X.-T. Wu, H. Lin and Q.-L. Zhu, *Chem. Mater.*, 2022, **34**, 3853-3861.
2. Y. Cheng, H. Wu, H. Yu, Z. Hu, J. Wang and Y. Wu, *Chem. Sci.*, 2022, **13**, 5305-5310.
3. N. Zhang, Q.-T. Xu, Z.-H. Shi, M. Yang and S.-P. Guo, *Inorg. Chem.*, 2022, **61**, 17002-17006.
4. H.-D. Yang, S.-H. Zhou, M.-Y. Ran, X.-T. Wu, H. Lin and Q.-L. Zhu, *Inorg. Chem. Front.*, 2023, **10**, 2030-2038.
5. N. Zhang, X. Huang, W.-D. Yao, Y. Chen, Z.-R. Pan, B. Li, W. Liu and S.-P. Guo, *Inorg. Chem.*, 2023, **62**, 16299-16303.